Investigation of the Behaviour of Gold Mesh Electrodes in Electrically Controllable Membrane Electrode Assemblies

C. Cosse[1*], M. Schumann[1], D. Becker[1] and D. Schulz[1]

[1]*Helmut Schmidt University / University of the Bundeswehr Hamburg, Holstenhofweg 85, 22043 Hamburg*

(*) carsten.cosse@hsu-hh.de

Introduction

Polymer electrolyte membrane fuel cells (PEMFC) are considered one of the most suitable energy converters to provide clean electricity for a plethora of applications [1, 2]. Especially in the field of mobile applications such as vehicles the demands on the specific power of the entire energy system as well as the requirements regarding the transient characteristics are very challenging. In order to achieve the steep load ramps in driving cycles, current PEMFCs need to be paired with batteries or super capacitors to compensate for the lacking responsiveness [3, 4]. The addition of these storage devices increases system cost, weight and complexity and is thus a significant detriment to widespread market introduction. To understand the lacking transient responsiveness, or rather the large time constant between two stationary operating points of PEMFC, the different transport processes occurring within each cell need to be understood. While the electrochemical reactions at the electrodes proceed in a similar timeframe as the processes within an electric grid, other processes such as the diffusion of educts and products to and from the catalytically active layers have relaxation times in the order of a few seconds [5], resulting in an unstable power supply. Previous work by this group proposed the addition of one or more electric field modifiers (EFM) within the membrane to selectively boost or attenuate the proton flux in the membrane [6].

Experimental Setup

Two electroformed gold meshes, with 750 lpi (MG44) and 2000 lpi (MG47) (Precision Eforming LLC.) and thicknesses of 8 and 5 µm respectively, are integrated into a membrane electrode assembly (MEA). The meshes are placed between two Nafion™ 212 membranes; two identical gas diffusion electrodes (0.5 mg/cm² 60 % Platinum on Vulcan – Sigracet 22BB) are used as anode and cathode. All components are bonded at 130 °C with a pressure of 400 N/cm² for three minutes in a polystat 200T (Servitec Maschinenservice GmbH). The MEA is then integrated into the quickCONNECTfixture qCf25 (balticFuelCells GmbH). A Greenlight Innovation G100 fuel cell test rig is used for operation and a prior preconditioning phase of 24 h (process parameters in Table 1). Figure 1 shows a schematic cross-section of the MEA and the corresponding electrical circuits of both fuel cell and EFM control, the latter of which is powered by a Gamry Reference 3000. To characterize the behaviour of the EFM, cyclic voltammetry (CV) measurements at three different operating potentials of the cell ($V_{\mathrm{Cell}} = 0.48, 0.40, 0.30\ V$) are conducted via constant current operation at various currents and facilitated by an electronic load (Höcherl & Hackl, PLI8006).

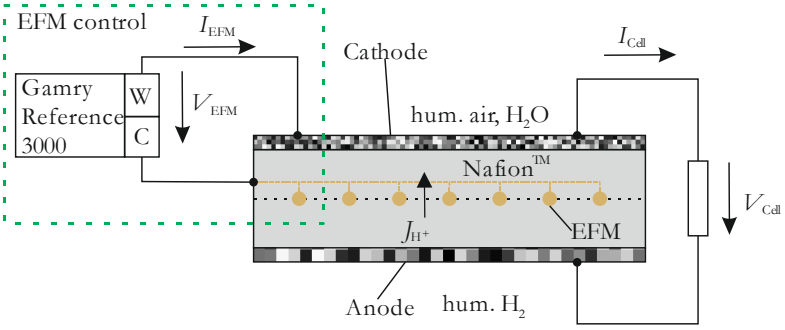

Figure 1. Schematic cross-section of the tested membrane electrode assemblies including the setup of the electrical circuits.

Table 1. Operating parameters of the experimental investigations

Parameter	Value	Unit
Temperature cell & gasses	60.0	°C
Temperature anode dew point	56.0	°C
Temperature cathode dew point	50.0	°C
Pressure gasses	1.0	atm
Flowrate anode	1.0	nlpm
Flowrate cathode	2.5	nlpm

Experimental Results

Contrary to expectation, the fuel cell current, I_{Cell}, for the prototype with the finer mesh (MG47) is higher than for the coarse mesh (MG44), indicating no increase of the ohmic resistance of the membrane due to a decrease in the transmission of the mesh. The potential of the EFM control circuit, V_{EFM}, is cycled between -1 and +1 V at a rate of 10 mV/s. The resulting current in the EFM control circuit, I_{EFM}, is measured and the resulting I-V-plots are shown in Figure 2a). All plots exhibit two distinct linear ranges with transition onsets at varying voltage values. For both types of mesh the voltage of the transition range is dependent on the operational voltage of the cell. With increasing cell voltage, the transition range shifts to higher voltages in the EFM circuit. For both prototypes the transition range begins at

voltages in excess of the operational voltage. This can also be seen in Figure 2b), where the cell voltage is plotted over the EFM voltage. Furthermore, the plots for the two different mesh types exhibit different gradients. While the negative current for the prototype with the coarser mesh remains very small due to a negative potential difference in the EFM control circuit, this characteristic changes for the finer mesh. Here, in both linear ranges below and above the transitional range the gradient of the I-V-plot is larger than for the coarse mesh. This seems to indicate a surface reaction at the EFM electrode. Since the surface area of the fine mesh is significantly larger as compared to the coarse mesh, a higher reaction rate is achieved leading to an increased current. At voltages exceeding the operational voltage, reduction reactions occur at the EFM, indicated by the positive current [7]. This could be due to hydrogen forming at or in the EFM [8]. Particularly for the fine mesh and less so for the coarse mesh, a negative current indicates oxidation reaction at the EFM. This could be linked to a hydrogen oxidation reaction with previously formed gas or water electrolysis. Figure 2b) shows some instability in the operation of the cell, most likely due to water droplets blocking the gas flow partly. Contrary to a configuration of a voltage source connected to the cell circuit in series, where a strictly proportional behaviour would be expected, a negative EFM voltage in the investigated range does not affect the cell voltage significantly.

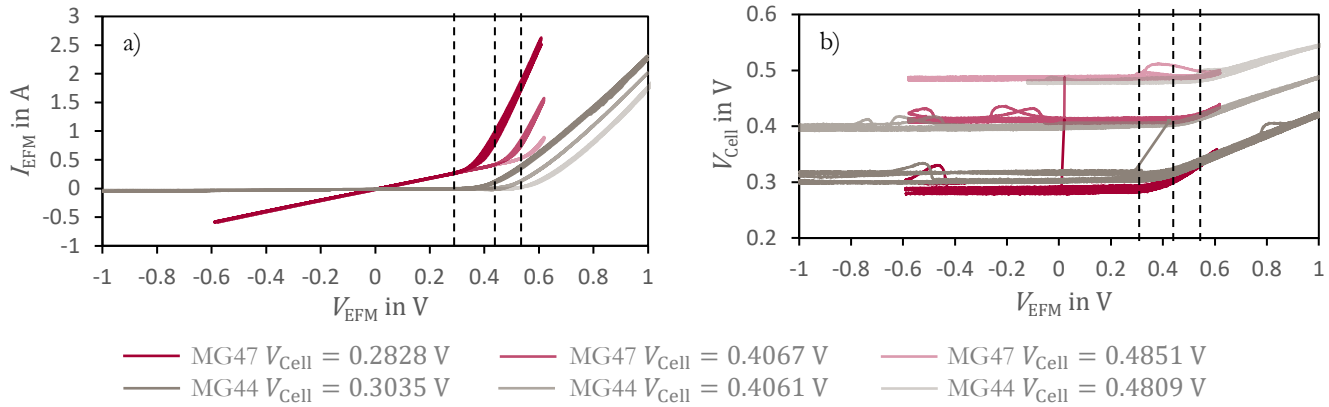

Figure 2. **a)** I-V-plot, and **b)** V-V-plot from the CV measurements for the MEAs with MG47 mesh (red lines) and MG44 mesh (grey lines). Black dashed indicator lines show the lower bound of the transition range.

Conclusion

It was shown that electroformed gold meshes can be integrated as EFM electrodes into a MEA without disrupting the regular fuel cell operation. In fact, cell voltage could be increased when voltages in excess of the operational voltage were applied. With an increased surface area of the EFM (finer mesh), less overpotential is required to increase the cell voltage. However, application of the finer mesh also led to an increase in the EFM circuit's current. Future investigations will focus on two aspects. First, utilisation of two EFM electrodes where the EFM circuit potential is independent from the fuel cell circuit; second, analysis of an increased hydrogen fraction in the cathode exhaust gas due to EFM operation.

Acknowledgement

The project *Development and Test of electrically controllable Membrane Units in Polymer Electrolyte Fuel Cells and Electrolysers with an internal Methanation in the gas exhaust pipe* is funded by the German Federal Ministry for Economic Affairs and Energy under the funding code 03ET6133A.

References

[1] T. Wilberforce et al., International Journal of Hydrogen Energy, vol. 42, no. 40, pp. 25695–25734, 2017, doi: 10.1016/j.ijhydene.2017.07.054.

[2] J. Garche and L. Jürissen, The Electrochemical Society Interface, vol. 24, pp. 39–43, 2015.

[3] F. Calili, M. S. Ismail, D. B. Ingham, K. J. Hughes, L. Ma, and M. Pourkashanian, International Journal of Hydrogen Energy, vol. 46, no. 33, pp. 17343–17357, 2021, doi: 10.1016/j.ijhydene.2021.02.133.

[4] X. Li, K. Han, and Song Yu, International Journal of Hydrogen Energy, vol. 45, no. 39, pp. 20312–20320, 2020, doi: 10.1016/j.ijhydene.2019.12.034.

[5] F. Grumm, M. Schumann, C. Cosse, M. Plenz, A. Lücken, and D. Schulz, Electronics, vol. 9, no. 4, p. 602, 2020, doi: 10.3390/electronics9040602.

[6] M. Schumann, F. Grumm, J. Friedrich, and D. Schulz, WSEAS TRANSACTIONS on CIRCUITS and SYSTEMS, vol. 18, pp. 55–62, 2019.

[7] Y. XU, International Journal of Hydrogen Energy, vol. 34, no. 1, pp. 77–83, 2009, doi: 10.1016/j.ijhydene.2008.09.090.

[8] M. G. Sustersic, N. V. Almeida, and A. E. von Mengershausen, International Journal of Hydrogen Energy, vol. 35, no. 11, pp. 6063–6068, 2010, doi: 10.1016/j.ijhydene.2009.12.068.